5328 *Chem. Mater.* **2010,** *22,* 5328–5332
DOI:10.1021/cm101671j

CHEMISTRY OF MATERIALS
Article

Synthesis, Structure, and Physical Properties of *A*-site Ordered Perovskites $ACu_3Co_4O_{12}$ (A = Ca and Y)

Ikuya Yamada,*[,†,§] Shintaro Ishiwata,[‡,¶] Ichiro Terasaki,[‡,⊥] Masaki Azuma,[†] Yuichi Shimakawa,[†] and Mikio Takano[†,△]

[†]*Institute for Chemical Research, Kyoto University, Uji, Kyoto 611-0011, Japan, and* [‡]*Department of Applied Physics, Waseda University, Tokyo 169-8555, Japan.* [§]*Current address: Department of Chemistry, Graduate School of Science and Engineering, Ehime University, 2-5 Bunkyo-cho, Matsuyama, Ehime 790-8577, Japan.* [¶]*Current address: Department of Applied Physics and Quantum-Phase Electronics Center (QPEC), University of Tokyo, Hongo, Tokyo 113-8656, Japan.* [⊥]*Current address: Department of Physics, Nagoya University, Furo-cho, Chikusa-ku, Nagoya 464-8602, Japan.* [△]*Current address: Institute for Integrated Cell-Material Sciences, Kyoto University, Yoshida Ushinomiya-cho, Sakyo-ku, Kyoto 606-8501, Japan.*

Received June 15, 2010. Revised Manuscript Received July 29, 2010

A-site ordered perovskites $CaCu_3Co_4O_{12}$ and $YCu_3Co_4O_{12}$, and their solid solutions $Ca_{1-x}Y_xCu_3Co_4O_{12}$ (x = 0.25, 0.50, and 0.75), were synthesized under high pressure (9 GPa) and high temperature (1273 K). They all have a $CaCu_3Ti_4O_{12}$-type structure (cubic, space group: $Im\bar{3}$) and the lattice constant a slightly decreased from 7.1226(5) Å of $CaCu_3Co_4O_{12}$ to 7.1195(3) Å of $YCu_3Co_4O_{12}$. Rietveld refinement based on synchrotron powder X-ray diffraction suggests that the valence state of $CaCu_3Co_4O_{12}$ is close to $CaCu^{3+}{}_3Co^{3.25+}{}_4O_{12}$, which differs from those of other $CaCu^{2+}{}_3B^{4+}{}_4O_{12}$ perovskites. Substitution of Ca with Y at the *A*-site changes the metallic $CaCu_3Co_4O_{12}$ to an insulating $YCu_3Co_4O_{12}$, and a metal−insulator transition occurs at $x = 0.50-0.75$. The electrical resistivity, thermoelectricity, and specific heat results reveal that electrons are doped into the Co 3d band and that the valence state changes from $CaCu^{3+}{}_3Co^{3.25+}{}_4O_{12}$ to $YCu^{3+}{}_3Co^{3+}{}_4O_{12}$.

Introduction

A-site ordered perovskites $AA'_3B_4O_{12}$ have been extensively studied recently for several interesting reasons.[1] They have remarkable electronic and magnetic properties, such as a large dielectric constant for $CaCu_3Ti_4O_{12}$,[2] large magnetoresistance in low magnetic fields for $CaCu_3Mn_4O_{12}$,[3] heavy-fermion-like behavior for $CaCu_3Ru_4O_{12}$ (CCRO),[4] ferromagnetism of Cu for $CaCu_3Ge_4O_{12}$ and $CaCu_3Sn_4O_{12}$,[5] and charge disproportionation for $CaCu_3Fe_4O_{12}$ (CCFO).[6] Substitutions at the *A*-site with aliovalent ions often induce drastic changes in the electronic structures of $ACu_3B_4O_{12}$. For instance, a substitution of Ca^{2+} with La^{3+} or Bi^{3+} changes the ferrimagnetic semiconductor of $CaCu_3Mn_4O_{12}$[3] to ferrimagnetic half metals of $LaCu_3Mn_4O_{12}$ or $BiCu_3Mn_4O_{12}$, respectively.[7,8] Similar substitution with La^{3+} or Bi^{3+} in CCFO changes the way of resolving its instability of the electronic structure.[9] CCFO, with an unusually high oxidation state of the Fe ions, shows charge disproportionation ($2Fe^{4+} \rightarrow Fe^{3+} + Fe^{5+}$),[6] whereas the substituted compounds $LaCu_3Fe_4O_{12}$ (LCFO)[10] and $BiCu_3Fe_4O_{12}$[11] show charge transfer ($3Cu^{2+} + 4Fe^{3.75+} \rightarrow 3Cu^{3+} + 4Fe^{3+}$).

In a $AA'_3B_4O_{12}$ structure, the relatively small and Jahn−Teller active ions such as Cu^{2+} (d^9) and Mn^{3+} (d^4) occupy 3/4 of the *A*-site with 4-fold planar coordination (= *A*′-site), while 1/4 of the *A*-site is occupied by ordinary alkaline, alkaline-earth, and rare-earth metals, with 12-fold coordination, as illustrated in the inset of Figure 1. A high pressure (several GPa) is often required for the synthesis of $AA'_3B_4O_{12}$ perovskites, presumably to stabilize such types of small cations at the *A*′-site. Here, given Ca^{2+} and Cu^{2+} at the *A*- and *A*′-sites, respectively, a quadrivalent transition-metal ion can be introduced into the *B*-site with 6-fold octahedral coordination. Considering the fact that

*Author to whom correspondence should be addressed. E-mail: ikuya@chem.sci.ehime-u.ac.jp.

(1) Shimakawa, Y. *Inorg. Chem.* **2008**, *47*, 8562.
(2) Ramirez, A. P.; Subramanian, M. A.; Gardel, M.; Blumberg, G.; Li, D.; Vogt, T.; Shapiro, S. M. *Solid State Commun.* **2000**, *115*, 217.
(3) Zeng, Z.; Greenblatt, M.; Subramanian, M. A.; Croft, M. *Phys. Rev. Lett.* **1999**, *82*, 3164.
(4) Kobayashi, W.; Terasaki, I.; Takeya, J.; Tsukada, I.; Ando, Y. *J. Phys. Soc. Jpn.* **2004**, *73*, 2373.
(5) Shiraki, H.; Saito, T.; Yamada, T.; Tsujimoto, T.; Azuma, M.; Kurata, H.; Isoda, S.; Takano, M; Shimakawa, Y. *Phys. Rev. B* **2007**, *B76*, 140403(R).
(6) Yamada, I.; Takata, K.; Hayashi, N.; Shinohara, S.; Azuma, M.; Mori, S.; Muranaka, S.; Shimakawa, Y.; Takano, M. *Angew. Chem., Int. Ed.* **2008**, *47*, 7032.
(7) Alonso, J. A.; Sánchez-Benítez, J.; De Andrés, A.; Martínez-Lope, M. J.; Casais, M. T.; Martínez, J. L. *Appl. Phys. Lett.* **2003**, *83*, 2623.
(8) Takata, K.; Yamada, I.; Azuma, M.; Takano, M.; Shimakawa, Y. *Phys. Rev. B* **2007**, *76*, 024429.
(9) Shimakwa, Y.; Takano, M. *Z. Anorg. Allg. Chem.* **2009**, *635*, 1882.
(10) Long, Y. W.; Hayashi, N.; Saito, T.; Azuma, M.; Muranaka, S.; Shimakawa, Y. *Nature* **2009**, *458*, 60.
(11) Long, Y. W.; Saito, T.; Tohyama, T.; Oka, K.; Azuma, M.; Shimakawa, Y. *Inorg. Chem.* **2009**, *48*, 8489.

 Published on Web 08/25/2010

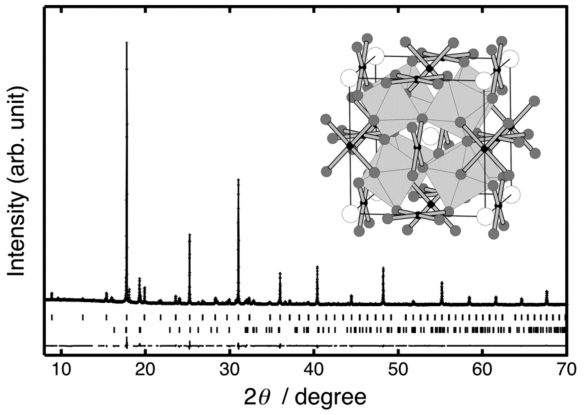

Figure 1. Observed synchrotron powder X-ray diffraction (SXRD) pattern and Rietveld refinement result for CCCO. The dots and lines indicate the observed and calculated patterns, respectively. The difference between the observed and calculated patterns is shown at the bottom. The top and bottom vertical marks indicate the Bragg reflection positions for CCCO, and CuO, respectively. The inset shows the crystal structure of $AA'_3B_4O_{12}$. Large white spheres, small black spheres with 4-fold planar coordination, and medium gray spheres represent A, A', and O atoms, respectively. The octahedra represent BO_6 octahedra.

a simple cobalt perovskite $SrCo^{4+}O_3$ already exists,[12] $CaCu_3Co_4O_{12}$ (CCCO) with Co^{4+} is the target synthesis.

In this article, we report a novel A-site ordered perovskite $CaCu_3Co_4O_{12}$ synthesized at 9 GPa and 1273 K. Structural refinement based on synchrotron powder X-ray diffraction (SXRD) data has revealed that the compound has an ionic composition of $Ca^{2+}Cu^{3+}{}_3Co^{3.25+}{}_4O_{12}$, rather than the expected $Ca^{2+}Cu^{2+}{}_3Co^{4+}{}_4O_{12}$. Magnetic susceptibility, electrical resistivity, thermoelectricity, and specific heat measurements demonstrate a drastic change in electronic properties when substituting Y for Ca in CCCO (from metallic CCCO to insulating $YCu_3Co_4O_{12}$ (YCCO)). The metal−insulator transition (MIT) is discussed in terms of the filling control of the Co 3d band.

Experimental Section

Polycrystalline samples of $Ca_{1-x}Y_xCu_3Co_4O_{12}$ ($x = 0.0$, 0.25, 0.50, 0.75, and 1.0) were prepared from stoichiometric mixtures of Y_2O_3 (99.9%), CuO (99.99%), Co_3O_4 (99.9%), and Ca_2CuO_3. Ca_2CuO_3 was synthesized in advance from a mixture of $CaCO_3$ (99.99%) and CuO (99.99%) at a molar ratio of 2:1 by firing at 1223 and 1273 K, respectively, in air for 24 h with occasional grinding. $KClO_4$, which is an oxidizing agent, was added, representing 25 wt % of the stoichiometric mixture. The mixture was placed into a gold capsule 2.8 mm in diameter, which was then placed into a pyrophyllite high-pressure cell with a graphite heater. The high-pressure cell was compressed to 9 GPa using a high-pressure apparatus. After compression, the capsule was heated to 1273 K in 5 min, held at this temperature for 30 min, and then quenched to room temperature. The applied pressure was released slowly after cooling. The polycrystalline sample was ground with a mortar, washed several times with distilled water, ethanol, and acetone (in this order), and then dried at 373 K in a dehydrator. The dense pellet required for electrical transport and specific heat measurements was prepared by sintering the washed powder at 9 GPa and 1273 K with $KClO_4$.

(12) Bezdicka, P.; Wattiaux, A.; Grenier, J. C.; Pouchard, M.; Hagenmuller, P. *Z. Anorg. Allg. Chem.* **1993**, *619*, 7.

Table 1. Refined Structure Parameters for $CaCu_3Co_4O_{12}$[a]

atom	site	g	x	y	z	$1000U$ (Å^2)
Ca	2a	1[b]	0	0	0	8.2(9)
Cu	6b	1[b]	0	$^1/_2$	$^1/_2$	4.4(3)
Co	8c	1[b]	$^1/_4$	$^1/_4$	$^1/_4$	0.8(2)
O	24g	1[b]	0.3076(2)	0.1765(2)	0	6.9(4)

[a] Space group $Im\bar{3}$ (No. 204), lattice constant $a = 7.12260(5)$ Å, $R_{wp} = 3.04\%$, $R_I = 2.71\%$, and goodness of fit $S_{fit} = 1.22$. [b] The site occupancy factor for all the atoms was fixed to 1.

Phase identification was determined in the powder X-ray diffraction (XRD) pattern using a Rigaku RINT 2500 system with Cu Kα radiation. The lattice constant a was refined by means of Rietveld analysis, using the Rietveld refinement program RIETAN-2000.[13] The crystal structure of CCCO was refined with RIETAN-2000 using the SXRD pattern collected by a Debye−Scherrer camera at the BL02B2 beamline of SPring-8.[14] The wavelength was resolved to 0.77711 Å against a CeO_2 standard. Thermogravimetry measurement was conducted from 300 K to 1200 K at a heating rate of 10 K min^{-1}, using a Rigaku ThermoPlus TG-8120 system.

Electrical resistivity measurement was carried out between 2 K and 300 K, using the standard four-probe method on a Quantum Design PPMS. Magnetic susceptibility on zero-field cooling (ZFC) and field cooling (FC) between 5 and 300 K in an external field of 10 kOe and isothermal magnetization at temperatures between 5 and 300 K were measured using a Quantum Design superconducting quantum interference device (SQUID) magnetometer (MPMS-XL). Measurement of the specific heat was conducted between 2 K and 20 K, using a relaxation method on the PPMS. Thermoelectric power was measured between 5 K and 280 K, using a steady-state method in a liquid He cryostat.

Results and Discussion

Almost single-phase samples of $Ca_{1-x}Y_xCu_3Co_4O_{12}$ ($x = 0.0-1.0$) were obtained at 9 GPa and 1273 K, although they were unavailable below this pressure. Small amounts of impurities such as CuO (~10 wt %) and unidentified phases were found in all of the samples.

The SXRD pattern of CCCO showed the cubic A-site ordered perovskite structure of the compound. The crystal structure refinement of CCCO was performed on the basis of the space group $Im\bar{3}$ (No. 204). Figure 1 shows the observed and calculated SXRD patterns of CCCO. Table 1 lists the structure parameters of CCCO obtained from the Rietveld refinement. It is difficult to determine whether the Co ions are incorporated into the A'-site because of the very similar atomic scattering factors of Co and Cu. Thus, for the first approximation, Co substitution for A'-site Cu was neglected. Since no significant oxygen deficiency was confirmed by thermogravimetric measurement, the occupancy factor (g) of each site was fixed to unity. The small values of the reliability factors (R_{wp} and R_I) and goodness-of-fit (S_{fit}) indicate satisfactory structure refinement, based on the above structure model. Selected bond lengths and angles of CCCO are listed in Table 2. Note that the shortest Cu−O bond length (~1.86 Å)

(13) Izumi, F.; Ikeda, T. *Mater. Sci. Forum* **2000**, *321−324*, 198.
(14) Nishibori, E.; Takata, M.; Kato, K.; Sakata, M.; Kubota, Y.; Aoyagi, S.; Kuroiwa, Y.; Yamakata, M.; Ikeda, N. *Nucl. Instrum. Methods Phys. Res., Sect. A* **2001**, *467−468*, 1045.

Table 2. Selected Bond Lengths and Bond Angles for $CaCu_3Co_4O_{12}$

	bond length (Å)		bond angle (°)
Ca−O (×12)	2.5262(18)	O−Cu−O	85.08(12)
Cu−O (×4)	1.8596(19)	O−Cu−O	94.92(11)
Cu−O (×4)	2.6807(19)	O−Co−O	89.78(8)
Co−O (×6)	1.9008(7)	O−Co−O	90.22(8)
		Co−O−Co	139.36(4)
		Cu−O−Co	110.20(5)

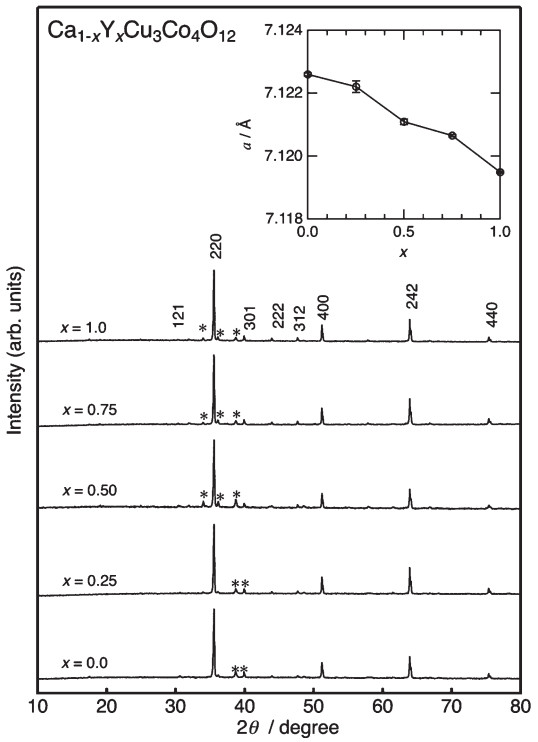

Figure 2. Cu Kα XRD patterns of $Ca_{1-x}Y_xCu_3Co_4O_{12}$. The asterisks represent the Bragg reflection positions of the impurity phases. The inset shows the lattice constant a, as a function of x.

is comparable to that of LCFO (~1.90 Å),[10] and that the bond valence sum (BVS)[15] of Cu was calculated to be 3.10.[16,17] The Co−O bond length (~1.90 Å) of CCCO is comparable to those of other cobalt perovskites containing Co^{3+} and Co^{4+} ions (e.g., ~1.93 Å for $LaCo^{3+}O_3$ and ~1.92 Å for $SrCo^{4+}O_3$),[12,18] but it is difficult to precisely estimate the oxidation state of the Co ion from the bond length. Given that Ca^{2+} and Cu^{3+} are the oxidation states in CCCO, the Co valence was closer to trivalent than quadrivalent, and the BVS of Co was calculated to be 3.14.[19,20] The BVS values of Cu and Co seemed to give a simple ionic composition, such as $CaCu^{3+}{}_3Co^{3.25+}{}_4O_{12}$, which is different from the initially expected ionic model of $CaCu^{2+}{}_3Co^{4+}{}_4O_{12}$. Although the Cu^{3+} ion is not Jahn−Teller active, a few compounds, such

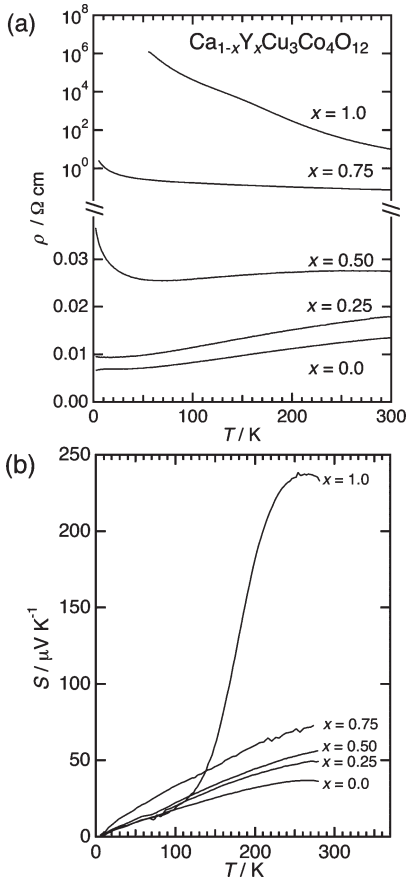

Figure 3. Temperature dependence of the (a) electrical resistivity and (b) thermoelectric power S for $Ca_{1-x}Y_xCu_3Co_4O_{12}$.

as $LaMn^{1.67+}{}_3Ti^{4+}{}_4O_{12}$ and $CaFe^{2+}{}_3Ti^{4+}{}_4O_{12}$, which contain non-Jahn−Teller ions at A'-site, were reported.[21,22] Thus, $CaCu^{3+}{}_3Co^{3.25+}{}_4O_{12}$ is another example in which non-Jahn−Teller ion is stabilized by high-pressure synthesis. The valence state of Cu^{3+} and $Co^{3.25+}$ (almost Co^{3+}) was confirmed by the photoemission study.[23]

Figure 2 shows the powder XRD data collected with Cu Kα radiation for $Ca_{1-x}Y_xCu_3Co_4O_{12}$ ($x = 0.0-1.0$). The $Ca_{1-x}Y_xCu_3Co_4O_{12}$ samples with $x \geq 0.25$ crystallize in the same crystal structure as CCCO. The lattice constant a monotonically decreases with increasing x, as shown in the inset of Figure 2. This is in contrast with the increase of a in $ACu_3B_4O_{12}$ (B = V and Ru), caused by the A-site substitution from Na^+ to Ca^{2+} to La^{3+} (or Y^{3+}),[24−26] in which the increase of a can be interpreted as the expansion of the BO_6 octahedron by electron doping. The substitution causes significant changes in electronic states of Co,

(15) Brown, I. D.; Altermatt, D. *Acta Crystallogr., Sect. B: Struct. Sci.* **1985**, *41*, 244.
(16) The BVS of Cu is calculated using the following parameters: b_0 = 0.37, r_0 = 1.738.
(17) Mahapatra, S.; Halfen, J. A.; Wilkinson, E. C.; Pan, G.; Wang, X.; Young, V. G., Jr.; Cramer, J. C.; Que, L., Jr.; Tolman, W. B. *J. Am. Chem. Soc.* **1996**, *118*, 11555.
(18) Radaelli, P. G.; Cheong, S.-W. *Phys. Rev. B* **2002**, *66*, 094408.
(19) The BVS of Co is calculated using the following parameters: b_0 = 0.37, r_0 = 1.661.
(20) Wood, R. M.; Palenik, G. J. *Inorg. Chem.* **1998**, *37*, 4149.
(21) Long, Y. W.; Saito, T.; Mizumaki, M.; Agui, A.; Shimakawa, Y. *J. Am. Chem. Soc.* **2009**, *131*, 16244.
(22) Leinweber, K.; Linton, J.; Navrotsky, A.; Fei, Y.; Parise, J. B. *Phys. Chem. Miner.* **1995**, *22*, 251.
(23) Mizokawa, T.; Morita, Y.; Sudayama, T.; Takubo, K.; Yamada, I.; Azuma, M.; Takano, M.; Shimakawa, Y. *Phys. Rev. B* **2009**, *80*, 125105.
(24) Shiraki, H.; Saito, T.; Azuma, M.; Shimakawa, Y. *J. Phys. Soc. Jpn.* **2008**, *77*, 064705.
(25) Labeau, M.; Bochu, B.; Joubert, J. C.; Chenavas, J. *J. Solid State Chem.* **1980**, *33*, 257.
(26) Ramirez, A. P.; Lawes, G.; Li, D.; Subramanian, M. A. *Solid State Commun.* **2004**, *131*, 251.

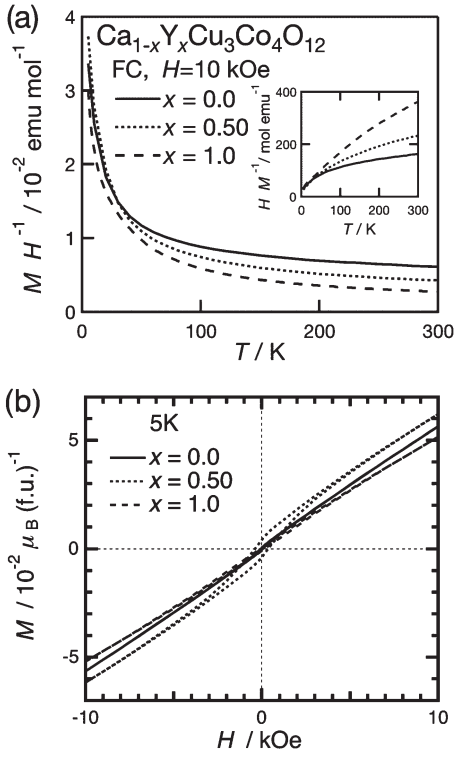

Figure 4. (a) Temperature dependence of the magnetic susceptibility measured in an external field of 1 0 kOe on FC for $Ca_{1-x}Y_xCu_3Co_4O_{12}$. The inset shows the temperature dependence of the inverse magnetic susceptibility. (b) Isothermal magnetization curve measured at 5 K for $Ca_{1-x}Y_xCu_3Co_4O_{12}$.

as discussed later. Thus, the relationship between the lattice constant and the doping level in the present system is not simple as we saw in the rigid-band doping.

Figure 3a shows the temperature dependence of the electrical resistivity. CCCO showed metallic temperature dependence with positive $d\rho/dT$ over the entire temperature range that has been measured. The metallic behavior was consistent with $CaCu^{3+}{}_3Co^{3.25+}{}_4O_{12}$ valence state with a partially filled Co t_{2g} band, obtained from BVS calculation. This result also confirmed that the $CaCu^{2+}{}_3Co^{4+}{}_4O_{12}$ valence state with a fully occupied Co t_{2g} band was not achieved. Also, the ρ value at room temperature increased by 3 orders of magnitude, from ~0.01 Ω cm for CCCO to ~10 Ω cm for YCCO. Insulator-like temperature dependence of ρ with negative $d\rho/dT$ was observed for $x \geq 0.75$. The drastic change in electrical resistivity indicated an MIT caused by electron doping. If YCCO also contains a Cu^{3+} state at the A'-site, then the substitution would change the valence state of Co from $Co^{3.25+}$ to Co^{3+}. Because of the spatially isolated CuO_4 unit, the Cu 3d electron probably makes little contribution to the electrical transport property, as discussed in LCFO.[10] Therefore, the insulating behavior of YCCO is explained by the full filling of electrons into the Co t_{2g} band. Thus, we conclude that the MIT from CCCO to YCCO is induced by filling control of the Co t_{2g} band. This interpretation was also confirmed by a photoemission study.[23]

Figure 3b shows the temperature dependence of the thermoelectric power (S). Positive values for all the composition indicated that a p-type conduction mechanism is dominant. The almost-linear temperature dependence of S agrees with the metallic conductivity observed in electrical resistivity for $x = 0.0-0.50$. In a simple metal model, S is proportional to $T/N(E_F)$, where $N(E_F)$ is the density of states at the Fermi level. Thus, the increase in S from $x = 0.0$ to $x = 0.75$ reflects the decrease in $N(E_F)$ after electron doping. In contrast, YCCO showed an anomalous temperature dependence of S. It is difficult to explain its mechanism, but the large S value and large temperature dependence differed from those of metallic samples, representing that the insulating transport property is dominant for $x = 1.0$.

Figure 4a shows the temperature dependence of the magnetic susceptibility of $x = 0.0$, 0.50, and 1.0 samples measured on FC in an external magnetic field of 10 kOe. There is no difference between ZFC and FC data, and no magnetic transition was observed in the measured temperature range of 5−300 K. Small ferromagnetic hysteresis loops were observed in the $M-H$ curve for all the samples, as shown in Figure 4b. The hysteresis loops were present over the entire temperature range and were temperature-dependent. This is probably attributed to unidentified ferromagnetic impurities. The magnetic susceptibility data of all the samples showed a Curie−Weiss (CW)-like paramagnetic behavior with involvement of the temperature-independent component, which was confirmed by the nonlinear shape of the inverse magnetic susceptibility, as shown in the inset of Figure 4a. The magnetic susceptibility data of CCCO and YCCO between 5 K and 300 K were analyzed by CW fitting: $\chi = C_{CW}/(T - \theta_w) + \chi_0$, where C_{CW} is the Curie constant, θ_w the Weiss temperature, and χ_0 the temperature-independent component. The C_{CW} values obtained from the fitting were 0.379(7) emu K mol^{-1} for CCCO and 0.560(5) emu K mol^{-1} for YCCO. Since the A'-site Cu ions were considered to be in the nonmagnetic Cu^{3+} (d^8, $S_{spin} = 0$) state from the structural analysis and photoemission spectroscopy,[24] a large part of the CW component is probably derived from unidentified paramagnetic impurities. The χ_0 for CCCO was $5.16(6) \times 10^{-3}$ emu mol^{-1} and the rather large value indicates Pauli-like paramagnetism. Thus, the itinerant Co 3d electrons contributed to the large χ_0 value. The χ_0 value decreased to $1.02(3) \times 10^{-3}$ emu mol^{-1} for YCCO, as would be expected by the decrease in hole-like carrier concentration by electron doping.

Figure 5 shows the specific heat divided by temperature ($C\,T^{-1}$) as a function of T^2. No indication of magnetic transition was confirmed for any of the compositions. A Schottky-type anomaly was observed below ~10 K, because of excitation of the nuclear moment of ^{59}Co. The data between 12 K and 20 K (T^2 = 144−400 K^2) were fitted using the formula

$$\frac{C}{T} = \gamma + \frac{12\pi^4}{5} N_A k_B T^2 \left(\frac{1}{\Theta_D{}^3}\right)$$

where γ is Sommerfeld coefficient, N_A Avogadoro's constant, and Θ_D the Debye temperature. The value of γ decreased from 157.5(7) mJ mol^{-1} K^{-2} for CCCO to

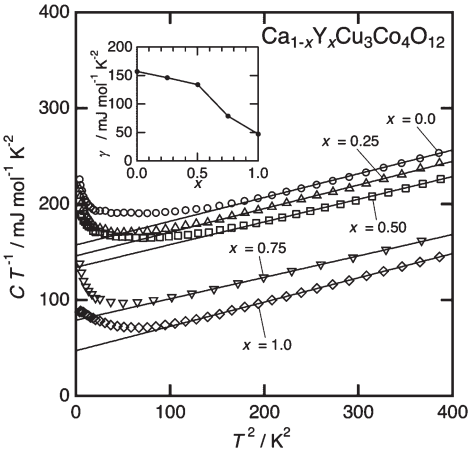

Figure 5. C/T as a function of T^2 for $Ca_{1-x}Y_xCu_3Co_4O_{12}$. The inset shows x dependence of γ.

47.26(13) mJ mol^{-1} K^{-2} for YCCO, as shown in the inset of Figure 5, while the Θ_D was almost unchanged at ~530 K. The decrease in γ clearly represents the decrease in $N(E_F)$, which agrees with the electrical transport and magnetic data. In particular, the sudden decrease in γ, as seen from $x = 0.50-0.75$ samples, corresponds to the MIT.

Structural analysis of CCCO revealed the valence state of $CaCu^{3+}{}_3Co^{3.25+}{}_4O_{12}$, and the evolution of the electrical transport and magnetic properties suggested that the substitution of Ca with Y caused electron doping into the Co t_{2g} band. Thus, the valence state of the A'-site Cu in a CCCO−YCCO solid solution does not seem to change from Cu^{3+}. This is in sharp contrast to the Cu^{2+} state in CCFO and the Cu^{3+} state in LCFO. The Cu^{3+} states in $Ca_{1-x}Y_xCu_3Co_4O_{12}$ are considered as states with ligand oxygen holes ($\underline{L}$), as in LCFO, and the ligand oxygen holes are located at the Cu−O hybridization bands, not at the Co−O bands. Thus, the $Cu^{3+}(d^9\underline{L})/Co^{3+}(d^6)$ state is more stable than the $Cu^{2+}(d^9)/Co^{4+}(d^6\underline{L})$ state.

The metallic transport property of CCCO was similar to those of other paramagnetic metal $CaCu_3B_4O_{12}$ (where B = V, Ru) perovskites. The large χ_0 and γ values were comparable to those of $CaCu_3V_4O_{12}$ (CCVO)[24] and CCRO.[4] This suggests that the electron mass is also enhanced in CCCO, probably because of the strong correlation of the Co 3d electrons. In CCVO and CCRO, metallic transport properties were observed through wide ranges of doping. In contrast, MIT was induced in $Ca_{1-x}Y_xCu_3Co_4O_{12}$ by electron doping. Thus, the aliovalent substitution at the A-site controlled the filling of the Co 3d band and led to MIT.

Conclusions

Novel A-site ordered perovskites $CaCu_3Co_4O_{12}$, $YCu_3Co_4O_{12}$, and their solid solutions $Ca_{1-x}Y_xCu_3Co_4O_{12}$ (x = 0.25, 0.50, and 0.75) were synthesized at 9 GPa and 1273 K; these crystallized in a cubic $CaCu_3Ti_4O_{12}$-type structure. The Rietveld refinement based on the synchrotron powder X-ray diffraction suggested that the valence state of $CaCu_3Co_4O_{12}$ is $CaCu^{3+}{}_3Co^{3.25+}{}_4O_{12}$, which differed from those of other $CaCu^{2+}{}_3B^{4+}{}_4O_{12}$ perovskites. The substitution at the A site from $CaCu_3Co_4O_{12}$ to $YCu_3Co_4O_{12}$ changed the filling of electrons into the Co 3d band and the filling-controlled MIT was induced at $x = 0.50-0.75$.

Acknowledgment. The authors thank Satoshi Shinohara, Shigeo Mori, and Takashi Mizokawa for fruitful discussion. This work was supported, in part, by the Grants-in-Aid for Scientific Research (Grant No. 19GS0307, 18350097, 17105002, 19014010, 19340098, 19052008, and for Joint Project of Chemical Synthesis Core Research Institute.) I. Y. was financially supported by 21COE on the Kyoto Alliance for Chemistry. The synchrotron radiation experiments were performed at SPring-8 with the approval of the Japan Synchrotron Radiation Research Institute.

Supporting Information Available: Crystallographic data of $CaCu_3Co_4O_{12}$ (in CIF format). This information is available free of charge via the Internet at http://pubs.acs.org/.